Journal of Hazardous Materials 164 (2009) 138–145

Contents lists available at ScienceDirect

Journal of Hazardous Materials

journal homepage: www.elsevier.com/locate/jhazmat

Characterization of TiO_2–Chitosan/Glass photocatalyst for the removal of a monoazo dye via photodegradation–adsorption process

Zulkarnain Zainal, Lee Kong Hui*, Mohd Zobir Hussein, Abdul Halim Abdullah, Imad (Moh'd Khair) Rashid Hamadneh

Chemistry Department, Faculty of Science, Universiti Putra Malaysia, 43400 UPM Serdang, Selangor Darul Ehsan, Malaysia

ARTICLE INFO

Article history:
Received 6 December 2007
Received in revised form 8 May 2008
Accepted 31 July 2008
Available online 13 August 2008

Keywords:
Photodegradation
Adsorption
Titanium dioxide
Chitosan
Visible light

ABSTRACT

In this paper, the newly explored TiO_2–Chitosan/Glass was suggested as a promising alternative material to conventional means of wastewater treatment. Characterization of TiO_2–Chitosan/Glass photocatalyst was studied with SEM-EDX, XRD, and Fourier transform infrared spectroscopy (FTIR) analysis. The combination effect of photodegradation–adsorption process for the removal of methyl orange (MO), an acid dye of the monoazo series occur promisingly when four layers of TiO_2–Chitosan/Glass photocatalyst was used for MO removal. Approximately, 87.0% of total MO removal was achieved. The reactive $-NH_2$, –OH, and metal oxide contents in the prepared photocatalyst responsible for the photodegradation–adsorption effect were confirmed by FTIR study. Similarly, MO removal behavior was well supported by SEM-EDX and XRD analysis. Significant dependence of MO removal on the TiO_2–Chitosan loading can be explained in terms of relationship between quantum yield of photocatalytic reactions and photocatalyst structure/activity. Hence, the research work done thus far suggests a new method, having both the advantages of photodegradation–adsorption process in the abatement of various wastewater pollutants.

1. Introduction

Recently, the arising ecological problems related to the pollution of water source have gained a lot of attention. One of the major sources of contaminants comes from the textile industries, in which its worldwide industry consumption is in excess of 10^7 kg/year and an estimated 90% of this ends up on fabrics [1]. Consequently, it is estimated that from 1 to 15% of the dyes used are lost in waste streams during synthesis and processing in the textile industry [1–5]. These wastewaters cannot be treated easily because their natural biodegradability has become increasingly difficult owing to the improved properties of dyestuffs. Indeed, dyes are designed to have a good fastness under typical usage conditions and thus, traditional wastewater treatment methods such as flocculation, activated carbon adsorption and biological treatment are increasingly ineffective [3,6–7].

Methyl orange which is a stable basic azo dye is a compound that contain azo groups (–N=N–) linked to methine or aromatic sp^2-hybridized C-atoms. The azo groups are mostly bound to benzene or naphthalene rings. Occasionally, they are also attached to aromatic heterocycles or to enolizable aliphatic groups. In view of its high stability, methyl orange is commonly used as titration indicator and staining agent [8]. Hence, it was chosen as a model pollutant in the present study.

Since the last three decades, heterogeneous photocatalytic oxidation process has been studied extensively for the destructive oxidation of various organic pollutants. Among a variety of photocatalysts employed, titanium dioxide (TiO_2) is the most preferable material due to its non-toxic, insoluble, stability, high photoactivity and inexpensive nature. It has been proven to be very effective, since many aromatic compounds can be degraded successfully to safer end products such as CO_2, H_2O, and mineral acids [6,9–11]. However, the use of TiO_2 together with chitosan has never been reported in any wastewater purification system. Adsorption process mediated by chitosan is one of the effective techniques that have been successfully employed for various pollutants (organic, inorganic, and heavy metal) removal from wastewater. It is in this regard that we would like to present here the combined effect of photodegradation–adsorption using the prepared thin film of TiO_2 and chitosan supported on glass (TiO_2–Chitosan/Glass) under the illumination of visible light as a new method for the treatment or pre-treatment of dye-containing wastewater.

The photocatalytic degradation of organic dyes in wastewater utilizing titanium dioxide (TiO_2, an n-type semiconductor) is initiated by light of wavelength $\lambda \leq 390$ nm (3.2 eV). Then, electrons

* Corresponding author. Tel.: +60 3 89466810; fax: +60 3 89435380.
E-mail addresses: zulkar@fsas.upm.edu.my (Z. Zainal), gs11613@hotmail.com (L.K. Hui).

0304-3894/$ – see front matter © 2008 Elsevier B.V. All rights reserved.
doi:10.1016/j.jhazmat.2008.07.154

are excited from the valence band to the conduction band, generating positive holes and free electrons. The produced electron–hole pairs can recombine or interact with other organic substrates on the surface of TiO_2 particles via the oxidation and reduction reactions. In aqueous solution, the positive holes are scavenged by surface hydroxyl groups to produce the very reactive oxidizing hydroxyl radicals ($^{\bullet}OH$), which can promote the degradation process and subsequently lead to the total mineralization of the organic substrate [12–16].

Recently, there are a few groups of researcher examining the degradation mechanism of several dyes under visible light or solar light irradiation. They had suggested a new method for the treatment or pre-treatment of dye-containing wastewater. The process is inspired by the principle of photosensitization of wide band gap semiconductors [5,17]. When a colored organic compound is present, the adsorbed dye molecule is excited by visible light, thus acts as a photosensitizer capable of injecting an electron into the conduction band of semiconductor particles to form an oxidized radical. The oxidized form of the dye molecules will then undergo further degradation. Detailed mechanism of dye degradation under visible light irradiation is described by Eqs. (1)–(6) [18–19]:

$$\text{Dye} + h\nu \rightarrow \text{Dye}* \quad (1)$$

$$\text{Dye}* + \text{TiO}_2 \rightarrow \text{Dye}^{\bullet+} + \text{TiO}_2(\text{e}) \quad (2)$$

$$\text{TiO}_2(\text{e}) + \text{O}_2 \rightarrow \text{TiO}_2 + \text{O}_2^{\bullet-} \quad (3)$$

$$\text{O}_2^{\bullet-} + \text{TiO}_2(\text{e}) + 2\text{H}^+ \rightarrow \text{H}_2\text{O}_2 \quad (4)$$

$$\text{H}_2\text{O}_2 + \text{TiO}_2(\text{e}) \rightarrow {}^{\bullet}\text{OH} + \text{OH}^- \quad (5)$$

$$\text{Dye}^{\bullet+} + \text{O}_2(\text{or}\,\text{O}_2^{\bullet-}\,\text{or}\,{}^{\bullet}\text{OH}) \rightarrow \text{peroxylated or hydroxylated intermediates} \rightarrow\rightarrow \text{degraded or mineralized products} \quad (6)$$

On the other hand, chitosan has been reported for the high adsorption potentials of dyes [20–22], metal ions [23–24], organic acids [24–25], and pesticide [26]. Other useful features of chitosan making it a versatile adsorbent include its abundance, non-toxicity, hydrophilicity, biocompability, biodegradability, and anti-bacterial property [27–29]. Chitosan [β-(1-4)-2-amino-2-deoxy-D-glucose] being a hydrolyzed derivative of chitin contains high amount of amino ($-NH_2$) and hydroxyl (OH) functional groups. In fact, both $-NH_2$ and –OH groups on chitosan chains can serve as coordination and reaction sites. Adsorption of organic substrates by chitosan is via the electrostatic attraction formed between the $-NH_2$ functional groups and the solutes. Whereas, the binding ability of chitosan for metal ion is attributed to the chelating groups (the $-NH_2$ and –OH groups) on the chitosan [24,28].

In our present study, chitosan was used as binder to anchor the reactive TiO_2 onto the smooth surface of glass plates. It will be very interesting to investigate the combined effect of photodegradation–adsorption mediated by TiO_2–Chitosan. The photocatalytic degradation process utilizing TiO_2 has been proven to be very effective for the degradation of various organic pollutants. However, it is ineffective for the abatement of heavy metal constituents as metal ions are generally non-degradable [30]. They have infinite lifetimes, and build up their concentrations in food chains to toxic levels. Contrarily, chitosan was known to have a very promising capability in this regard. Therefore, it was expected that TiO_2 and chitosan can complement each other with their own advantages, hence, providing a comprehensive method in the abatement of various wastewater pollutants.

2. Experimental details

2.1. Materials

The photocatalyst employed was commercial titanium dioxide supplied by Degussa (P25), Jebsen & Jessen Industrial (Malaysia) Sdn. Bhd. According to the manufacturer's specifications, P25 has an elementary particle size of 30 nm, BET surface area, ca. 50 m^2/g and its crystalline mode is 80% anatase and 20% rutile. Chitosan [β-(1-4)-2-amino-2-deoxy-D-glucose] with ≥80% of deacetylation degree and high molecular weight was supplied by TCI Co. Ltd., Tokyo, Japan. Schematic representation of chitosan structure is shown in Fig. 1. Methyl orange (MO), (4-[4-(dimethylamino)-phenylazo] benzenesulfonic acid, sodium salt), M = 327.34 g/mol, ~85% dye content was purchased from BDH Laboratory Supplies in England and its chemical structure is illustrated in Fig. 2 [31]. Acetic acid (CH_3COOH) and sodium chloride (NaCl) used to dissolve chitosan were of analytical grade. All the reagents were used as received without further purification. Deionized (DI) water produced from Millipore Alpha Q system was used to prepare all solutions in the study.

2.2. Preparation of TiO_2–Chitosan coated glass (TiO_2–Chitosan/Glass) photocatalyst

Two typical procedures for the preparation of TiO_2–Chitosan catalyst were applied: 2.5 g of chitosan flake was dissolved in a premixed solution of 300 ml (0.1 M) CH_3COOH and 40 ml (0.2 M) NaCl. The viscous solution was stirred continuously for 12 h to fully dissolve the chitosan flake. Then, 2.5 g of TiO_2 Degussa P-25 powder was added into the viscous solution. Subsequently, another 50 ml of (0.1 M) CH_3COOH was added. The slurry was stirred continuously for 24 h to obtain the final transparent viscous solution. The second procedure is the same as the initial, with difference in the mass of TiO_2 Degussa P-25 powder being used (25.0 g).

Pieces of 45 mm × 80 mm × 2 mm glass plates were used as support to immobilize the prepared TiO_2–Chitosan catalyst. The glass plates were first degreased, cleaned thoroughly and dried before deposition. Then, the glass plates were dipped in the viscous solution with a uniform pulling rate manually. The readily dipped glass plates were dried at 100 °C inside an oven for 4 h alternately after each dipping process. Dipping repetition was done as desired (from one layer to six layers). Herein, the synthesized samples are called TiO_2–Chitosan/Glass photocatalyst. TiO_2–Chitosan thin film

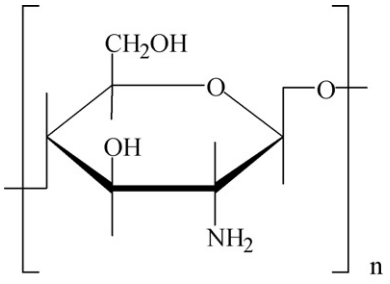

Fig. 1. Schematic representation of chitosan structure.

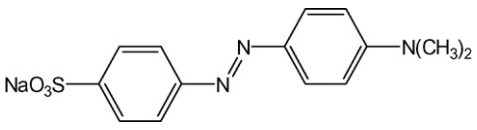

Fig. 2. Illustration of MO chemical structure.

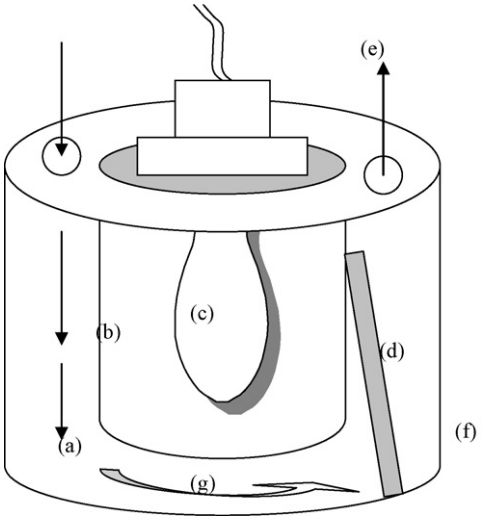

Fig. 3. Experimental set-up of the photodegradation–adsorption process.

formed on the glass plates was responsible for the photodegradation and adsorption reaction. Otherwise, the photocatalysts were stored in the dark to avoid pre-activation by room light or sunlight.

2.3. Characterization of TiO_2–Chitosan/Glass photocatalyst

Surface morphology of the TiO_2–Chitosan/Glass was studied by scanning electron microscope fitted with energy dispersive X-ray Spectrometer (SEM-EDX) analysis—LEO 1455 VPSEM and Oxford INCA EDX. Small pieces of the prepared photocatalyst were stuck on stubs using double-sided tape. Before the samples were analyzed, they were sputtered with a layer of gold film to prevent the occurrence of charging effect. Whereas, the phase composition of the prepared photocatalyst was studied using the powder and plate XRD technique. The patterns were recorded on a Shimadzu X-ray Diffractometer (XRD-6000) using Cu Kα radiation. Diffraction patterns were taken over the 2θ range 5–60°. Fourier transform infrared spectroscopy (FTIR) spectra of the precursor materials, TiO_2 Degussa P-25 powder, chitosan flake, and the prepared dried TiO_2–Chitosan catalyst were obtained ex-situ employing PerkinElmer Spectrometer FTIR Model 1725 X and a KBr beam splitter within wavelength range of 400.0–4000.0 cm^{-1}.

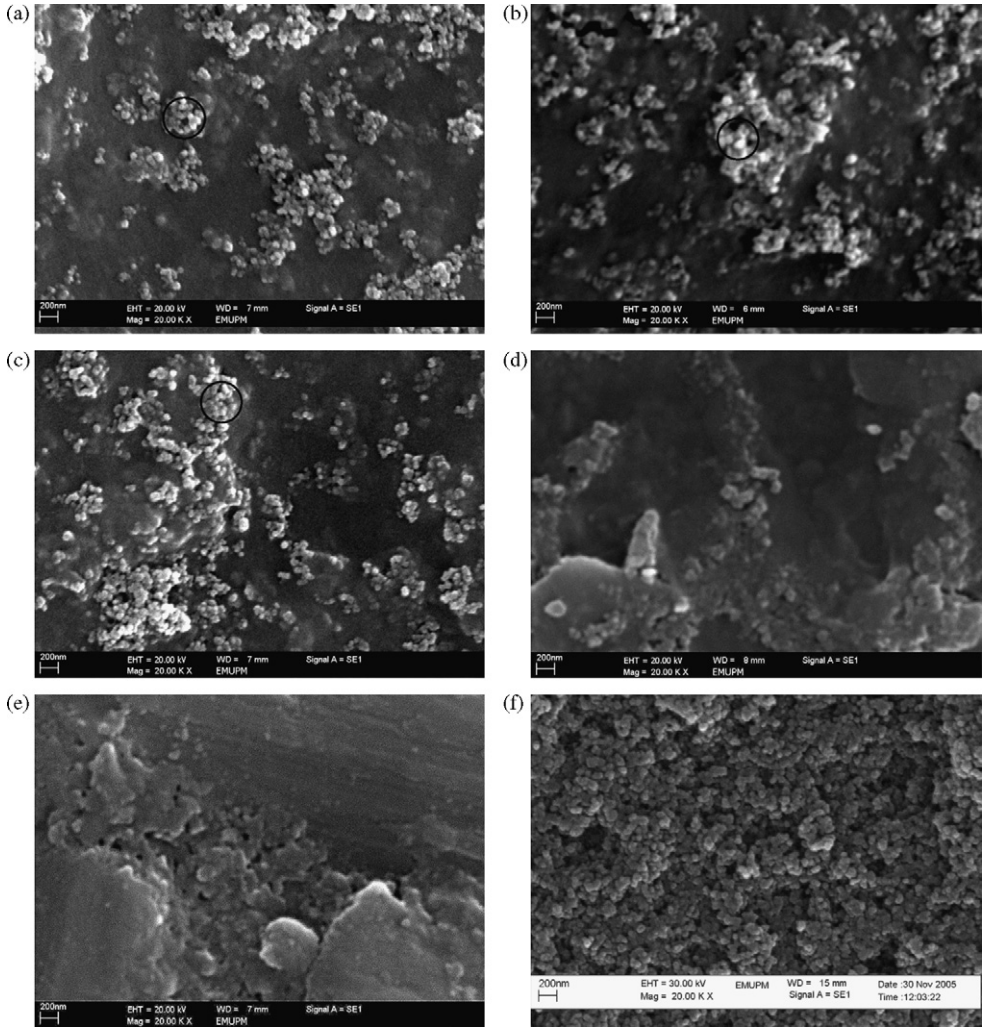

Fig. 4. SEM-EDX micrographs of TiO_2–Chitosan/Glass with different photocatalyst loading, 20,000×: (a) one layer; (b) two layers, (c) three layers, (d) four layers, (e) five layers, and (f) four layers/25.0 g of TiO_2 Degussa P-25.

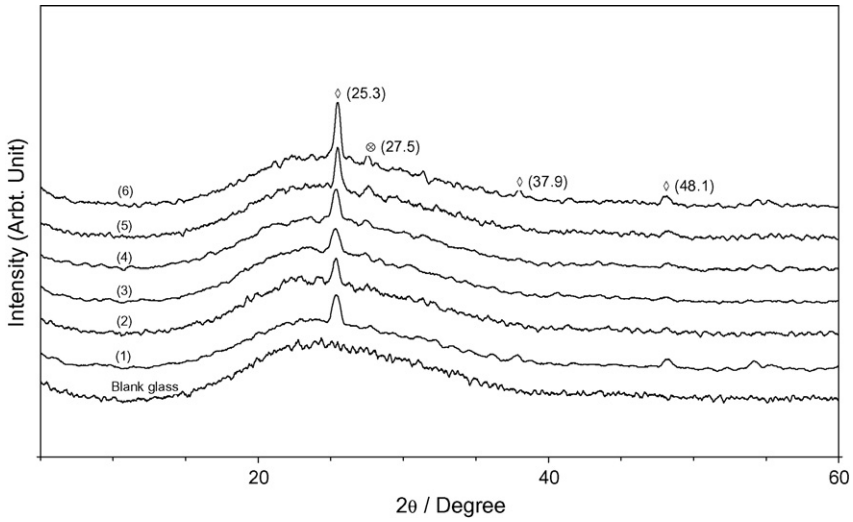

Fig. 5. X-ray diffraction patterns of TiO_2–Chitosan/Glass (2.5 g chitosan:2.5 g TiO_2 Degussa P-25) with different, photocatalyst loading (one to six dip-coating layers).

2.4. MO removal via photodegradation–adsorption reaction

The experiments were carried out in a custom made photodegradation–adsorption reactor as illustrated in Fig. 3. Five pieces of TiO_2–Chitosan/Glass with different number of dip-coating from 1 to 6 were used as photocatalyst. The solution was illuminated with a 15 W Philips white fluorescent light source at the centre of the solution reservoir, covered and separated by cylindrical quartz glass housing. Air was bubbled through the reaction solution to ensure a constant supply of oxygen and to give agitation effect to achieve equilibrium state of model pollutant-photocatalyst. Natural pH was applied for all of the experiments.

In a typical experiment, 1000 ml of MO with initial concentration of approximately 20 ppm was used as the model pollutant. Five milliliters of the samples were taken at regular interval and analyzed by PerkinElmer Lambda 20 UV–vis spectrometer to measure the temporal changes of MO concentration. The determination wavelength is 464.0 nm, which is the maximum absorption wavelength of MO as detected by UV–vis spectrometer.

3. Results and discussion

3.1. Surface morphology of TiO_2–Chitosan/Glass

SEM-EDX micrographs of TiO_2–Chitosan/Glass with a ratio of 1:1 (2.5 g of chitosan:2.5 g of TiO_2 Degussa P-25) and different photocatalyst loading (one dip-coated layer to six dip-coated layers) are shown in Fig. 4a–e, respectively. Macroreticular structure with spherical primary TiO_2 particles (as circled in Fig. 4a–c, respectively) of about 5–20 nm can be clearly seen. EDX analysis (results not shown here) [32] confirms that they were TiO_2 particles with the atomic ratio of titanium to oxygen of ca. 1:2. This suggests that TiO_2 were coated on the surface area of the prepared photocatalyst via chitosan as the bonding medium. While allowing the chitosan to react via adsorption mechanism, surface TiO_2 can be excited with light illumination of suitable wavelength ($\lambda < 390$ nm or $E_{bg} = 3.2$ eV) [4,6,11,17–18]. However, TiO_2 particles cannot be seen in Fig. 4d and e as they submerged into the coated layers of TiO_2–Chitosan/Glass. As observed, surface TiO_2 particles increase with increasing dip-coated layers. Subsequent increase of dip-coated layers after 3 will cover surface TiO_2 particles with dissolved chitosan. Hence, it is expected that photodegradation process will play a major role in one to three dip-coated layers of TiO_2–Chitosan/Glass, whereas MO removal will predominantly be attributed to adsorption process with subsequent increase of dip-coating layers.

Rationally, Fig. 4f shows that with an increase in TiO_2 precursor material (25.0 g of TiO_2 Degussa P-25) in the preparation of TiO_2–Chitosan catalyst, macroreticular structure of TiO_2 particles observed on the surface area of TiO_2–Chitosan/Glass increased tremendously and concurrently. It had covered up the whole surface area. This may suggest that a significant increase in MO removal via photodegradation process can be expected as more active surface area of TiO_2 particles was available for the reaction.

3.2. XRD analysis

XRD analysis was carried out to confirm the TiO_2 polymorphs and their crystalline phases. Fig. 5 shows the X-ray diffraction patterns of TiO_2–Chitosan/Glass with different photocatalyst loading (dip-coating layers). The peaks corresponding to the anatase TiO_2 phase appeared at $2\theta = 25.3°$, 37.9°, and 48.1°, respectively. As observed in Fig. 5, the major phase of TiO_2–Chitosan/Glass with different photocatalyst loading were predominantly anatase matching the standard JCPDS value. The peaks were getting sharper with increasing dip-coating layers. This indicates that photocatalyst loading has a significant effect on the TiO_2–Chitosan/Glass crystallinity. Higher intensity of TiO_2 peak shows that the availability of

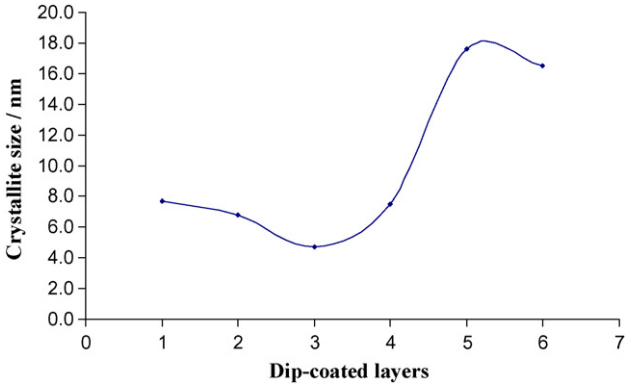

Fig. 6. Crystallite size of TiO_2 particles in TiO_2–Chitosan/Glass (2.5 g chitosan:2.5 g TiO_2 Degussa P-25) with different photocatalyst loading (one to six dip-coating layers).

TiO_2 compound increases as well, which is a favorable factor in the photodegradation process of organic compound. Co-existence of anatase and rutile (27.5°) peaks were only evident in the photocatalyst with five or more dip-coating layers. However, the existence of rutile phase may be detrimental to the photoactivity as rutile has been reported to be connected to its fast recombination rate of generated electron and holes [33].

The average crystallite sizes of TiO_2 were calculated by Scherrer's equation using the full width at half maximum (FWHM) of the X-ray diffraction peaks at $2\theta = 25.3°$ corresponding to the most intense anatase peak. Fig. 6 reveals that typical values of anatase crystallite size as calculated using Scherrer's equation were in the range of 4–18 nm for the synthesized TiO_2 particles in TiO_2–Chitosan/Glass. TiO_2 particles crystallite size as studied from XRD analysis was in well agreement with the SEM-EDX results discussed in Section 3.1 and with some of the reported results of other researchers [3,34–35]. The average anatase crystallite size of TiO_2 decreased slowly with the increase in photocatalyst loading from one to three layers. However, rapid increase of the crystallite size was observed with further increase in photocatalyst loading from four to six layers. An applause suggestion from the changing trend is that smaller crystallite size of TiO_2 particles with three to four dip-coating layers may yield more reaction surface area as rationalized with the large quantity of surface TiO_2 particles confirmed by SEM-EDX analysis in one to three dip-coated photocatalyst.

3.3. FTIR spectra of TiO_2–Chitosan/Glass

FTIR spectroscopy provides information on the nature of the precursor materials used and both the newly synthesized TiO_2–Chitosan catalyst. FTIR spectra for chitosan, TiO_2 Degussa P-25, and both dried TiO_2–Chitosan catalyst with different ratio were presented in Fig. 7. Absorption band of chitosan at 1640 cm^{-1} and 3436 cm^{-1} were attributed to its amine ($-NH_2$) and hydroxyl (–OH) functional groups [22,36]. Both of these functional groups on chitosan chains can serve as coordination and reaction sites for the adsorption of transition metals and organic species [28–29]. Fig. 7 also confirms the existence of metal oxide (TiO_2) at 656 cm^{-1} for TiO_2 Degussa P-25. However, absorption band for both the synthesized TiO_2–Chitosan catalyst shows an intrigue characteristic of both chitosan and TiO_2. Absorption spectra at 1410, 1566, 2852, 3436, and 3732 cm^{-1} were due to the banding of hydroxyl groups, in which hydroxyl band at 2852 cm^{-1} is a characteristic of surface TiO_2–OH functional group. On the other hand, absorption band at 1254, 1318, and 1640 cm^{-1} were attributed to the amine or amide functional groups. Appearance of band at 656 cm^{-1} reaffirms the existence of TiO_2 compound.

The significant increase of bands centred at 2920 and 2852 cm^{-1} may be attributable to the increase of TiO_2 used in the preparation of catalyst from 2.5 to 25.0 g. It is worth noting that FTIR spectra of both the synthesized TiO_2–Chitosan catalyst shows more peaks with higher intensities as compared to the precursor TiO_2 and chitosan. It indicates the enhancement of FTIR detection possibility when the samples were consisted of both the precursor materials. Besides, apparent existence of amine, amide, and hydroxyl functional groups together with TiO_2 metal oxide should help to confirm the effective removal of MO through photodegradation–adsorption process.

3.4. MO removal via photodegradation–adsorption process

A series of experiments were carried out to investigate the optimum catalyst loading for MO removal by varying the number of dip-coating from one to six layers. Blank experiments used as a control established that MO did not photodegrade when irradiated with visible light in the absence of photocatalyst. Removal of model pollutant attributable to adsorption effect was obtained when the experiments were run in the dark. Percentage removal due to adsorption effect was calculated as follows:

$$\%\ \text{removal of model pollutant} = \left[\frac{C_0 - C_t}{C_0}\right] \times 100 \quad (7)$$

where C_0 = concentration of model pollutant at 0 min, C_t = concentration of model pollutant at experimental time, t.

When the experiments were run under the illumination of a light source applying the same condition as for the experiment run in the dark previously, it represents the total removal of the model

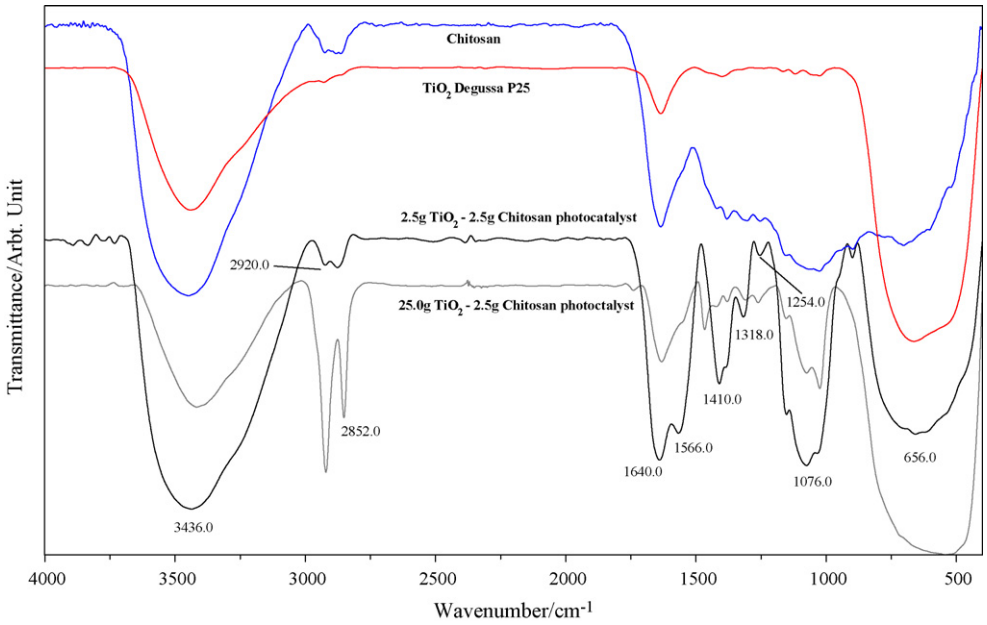

Fig. 7. FTIR spectra of chitosan, TiO_2 Degussa P25, and dried TiO_2–Chitosan (2.5 g and 25.0 g TiO_2).

Table 1
Effect of TiO_2–Chitosan loading on the photodegradation rate of MO

	Control/without photocatalyst	Dip-coated layers						
		1	2	3	4 (2.5 g TiO_2)	4 (25.0 g TiO_2)	5	6
K_{app} ($\times 10^{-3}$ min^{-1})	1.6	149.1	128.1	228.2	269.1	1203.9	187.4	161.3
Photodegradation (%)	≈0.0	6.8	12.9	29.7	33.7	28.0	12.8	0.67

pollutant which is inclusively due to both photodegradation and adsorption effect. Therefore, the difference in the removal between experiment carried out in the dark and under the illumination of a light source is a representation of model pollutant removal by photodegradation process. It can be simplified as follows:

photodegradation removal of model pollutant

= total removal under light illumination − removal in the dark (8)

Percentage removal due to photodegradation effect can be calculated as follows:

$$\%\ \text{removal of model pollutant (photodegradation)} = \left(\frac{C_{Pt}}{C_0}\right) \times 100\% \quad (9)$$

where C_0 = concentration of model pollutant at 0 min, C_{Pt} = concentration of model pollutant at experimental time, t removed by photodegradation effect.

In order to investigate the photodegradation and adsorption mechanism for the removal of MO based on the effect of TiO_2–Chitosan catalyst loading (layers), the pseudo first-order adsorption models were used. The photodegradation and adsorption of model pollutants can be well described by the Langmuir–Hinshelwood (L–H) kinetic model [37–39]. The rate of a unimolecular surface reaction, R is proportional to the surface coverage, θ and will follow Eqs. (10) or (11), respectively, when the reactant is more strongly adsorbed on the surface than the products

$$R = -\frac{dC}{dt} = k_r\theta = \frac{k_r K C_0}{1 + KC_0 + K_s C_s} \quad (10)$$

$$R = -\frac{dC}{dt} = k_r\theta = \frac{k_r K C_0}{1 + KC_0} \quad (11)$$

where k_r = reaction rate constant, θ = fraction of the surface covered by the reactant, K = adsorption coefficient of the reactant, C_0 = initial concentration of the reactant, K_s = adsorption coefficient of the solvent, C_s = concentration of the solvent.

Eq. (10) can be applied when both the reactant and the solvent compete for the same active sites, while Eq. (11) is only applicable when both the reactant and solvent are adsorbed on the surface without competing for the same active sites. Integration of Eqs. (10) and (11) yields Eqs. (12) and (13), respectively:

$$\ln\frac{C_0}{C} + \frac{K}{1 + K_s C_s}(C_0 - C) = \frac{k_r K}{1 + K_s C_s} t \quad (12)$$

$$\ln\frac{C_0}{C} + K(C_0 - C) = k_r K t \quad (13)$$

when C_0 is very small, Eqs. (12) and (13) reduce to Eqs. (14)

$$\ln\frac{C_0}{C} = k_{app} t \quad (14)$$

A plot of $\ln(C_0/C)$ vs. irradiation time should give a straight line whose slope represents the apparent first order rate constant, k_{app}. If a plot of $\ln(C/C_0)$ vs. irradiation time was plotted instead, the same graph was also attained but in the opposite plane (negative value).

When

$$\frac{C_0}{C} = 0.5, \qquad t_{1/2} = \frac{0.693}{k_{app}} \quad (15)$$

Half-life, $t_{1/2}$ is a useful indication of the rate of a first order chemical reaction of a substances. It describes the time taken for the concentration of a reactant to fall to half of its initial value.

The apparent rate constant, k_{app} of MO photodegradation is presented in Table 1. It is seen that the apparent rate constant increases with TiO_2–Chitosan loading up to four layers. Above four layers, subsequent increase of coating thickness had limited the absorption and penetration capability of light source. Thus, surface TiO_2 particles were not irradiated sufficiently, prompting the decrease in the rate constant value. The results presented here were well supported by the SEM-EDX and XRD analysis discussed earlier. Maximum surface TiO_2 particles were observed in SEM-EDX micrograph with three dip-coating layers. Similarly, TiO_2 crystallite size was the smallest at the interchange of three to four dip-coating layers as confirmed by XRD analysis, indicating the highest value of reactive surface area available. This trend had been observed by the other researchers as well [34,38–40] and can be explained by the fact that as the catalyst film becomes too thick, TiO_2 particles begin to mask itself effectively with the total irradiation being absorbed by only the initial layers of coated catalyst.

Comparatively, Table 2 shows the rate constant of MO adsorption. Interestingly, adsorption capability increases with increasing TiO_2–Chitosan loading from one layer (15.7×10^{-3} min^{-1}) to six layers (226.6×10^{-3} min^{-1}). It is evident that adsorption capability of chitosan had not reached its maximum limit. Examination of the data presented in Tables 1 and 2 may suggest that combination effect of photodegradation–adsorption by four layers of TiO_2–Chitosan/Glass is more preferable as the highest value of MO photodegradation was obtained. Although total removal of MO is the highest using six layers of TiO_2–Chitosan/Glass, MO removal by adsorption is by means of transferring it to another waste medium which is not the much desired wastewater treatment solution.

Tables 1 and 2 also show that by increasing the TiO_2:Chitosan ratio from 2.5 to 25.0 g of TiO_2, rate constant for both the photodegradation and adsorption process have been enhanced significantly by approximately four times higher. Total combination removal of MO also increased from 47.9 to 87.0% (four layers) in

Table 2
Effect of TiO_2–Chitosan loading on the adsorption rate of MO

	Control/without photocatalyst	Dip-coated layers						
		1	2	3	4 (2.5 g TiO_2)	4 (25.0 g TiO_2)	5	6
K_{app} ($\times 10^{-3}$ min^{-1})	1.6	15.7	47.4	57.9	80.7	638.3	163.2	226.6
Photodegradation (%)	≈ 0.0	1.9	4.5	11.2	14.2	59.0	44.6	64.6

which photodegradation efficiency had been maintained while at the same time adsorption capability was improved remarkably. As the ratio of chitosan used in the preparation of TiO_2–Chitosan catalyst remained the same (2.5 g), it may suggest that part of the adsorption capability was attributable to the increase of TiO_2 itself. This is in view that TiO_2 particles surface are mainly oxygen atoms with a high electron density (negative centres). Hence, TiO_2 particles have a negative charge and should, therefore, more readily adsorb MO which is a cationic molecule [41].

4. Conclusion

It is evident that the newly prepared TiO_2–Chitosan/Glass is capable of removing the model pollutant via the combined effect of photodegradation–adsorption. The reactive $-NH_2$, –OH, and metal oxide contents in the prepared TiO_2–Chitosan/Glass responsible for the photodegradation–adsorption effect were confirmed by FTIR study. Similarly, MO removal behavior was well supported by SEM-EDX and XRD analysis.

The obtained results also indicate that catalyst loading plays an important role in determining the removal efficiency of MO attributable to both photodegradation and adsorption process. Thus, optimum TiO_2–Chitosan catalyst coating must be applied to achieve maximum absorption of incident light for the excitation of surface TiO_2 particles. Better photodegradation effect was chosen instead of adsorption effect.

The research work done thus far suggests a new method, having both the advantages of photodegradation–adsorption process in the abatement of various wastewater pollutants. A ratio of 25.0 g TiO_2 Degussa P25:2.5 g Chitosan was chosen for further studies. The effect of initial concentration, photocatalyst heat-treatment, light intensity, and pH dependence on the photodegradation–adsorption process of the prepared TiO_2–Chitosan/Glass will be studied to apprehend a comprehensive understanding of the newly prepared photocatalyst, thus, further enhance its photodegradation–adsorption efficiency. In addition, the end products and intermediates produced during the photodegradation–adsorption process will be determined and investigated to ensure that no undesirable harmful or hazardous compounds were formed.

Acknowledgements

The authors greatly acknowledge NSF scholarship and IRPA funding with the number 09-02-04-0255-EA001 under the Ministry of Science, Technology and Innovation of Malaysia.

References

[1] Y.C. Wong, Y.S. Szeto, W.H. Cheung, G. McKay, Adsorption of acid dyes on chitosan-equilibrium isotherm analyses, Process Biochem. 39 (2004) 693–702.
[2] C. Bauer, P. Jacques, A. Kalt, Photooxidation of an azo dye induced by visible light incident on the surface of TiO_2, J. Photochem. Photobiol. A: Chem. 140 (2001) 87–92.
[3] Y. Chen, K. Wang, L. Lou, Photodegradation of dye pollutants on silica gel supported TiO_2 particles under visible light irradiation, J. Photochem. Photobiol. A: Chem. 163 (2004) 281–287.
[4] T. Sauer, G.C. Neto, H.J. José, R.F.P.M. Moreira, Kinetics of photocatalytic degradation of reactive dyes in a TiO_2 slurry reactor, J. Photochem. Photobiol. A: Chem. 149 (2002) 147–154.
[5] M. Stylidi, D.I. Kondarides, X.E. Verykios, Pathways of solar light-induced photocatalytic degradation of azo dyes in aqueous TiO_2 suspensions, Appl. Catal. B: Environ. 40 (2003) 271–286.
[6] C. Galindo, P. Jacques, A. Kalt, Photochemical and photocatalytic degradation of an indigoid dye: a case study of acid blue 74 (AB74), J. Photochem. Photobiol. A: Chem. 141 (2001) 47–56.
[7] A. Piscopo, D. Robert, J.V. Weber, Influence of pH and chloride anion on the photocatalytic degradation of organic compounds. Part I. Effect on the benzamide and para-hydroxybenzoic acid in TiO_2 aqueous solution, Appl. Catal. B: Environ. 35 (2001) 117–124.
[8] H. Zollinger, Color chemistry: syntheses, properties, and applications of organic dyes and pigments, Third revised edition, Wiley-VCH Gmbh & Co. KGaA, Weinheim and Verlag Helvetica Chimica Acta AG, Zürich, 2003, pp. 165–364.
[9] D. Chatterjee, A. Mahata, Visible light induced photodegradation of organic pollutants on dye adsorbed TiO_2 surface, J. Photochem. Photobiol. A: Chem. 153 (2002) 199–204.
[10] C. Galindo, P. Jacques, A. Kalt, Photodegradation of the aminoazobenzene acid orange 52 by three advanced oxidation processes: UV/H_2O_2, UV/TiO_2 and VIS/TiO_2. Comparative mechanistic and kinetic investigations, J. Photochem. Photobiol. A: Chem. 130 (2000) 35–47.
[11] R.W. Matthews, Photooxidation of organic impurities in water using thin films of titanium dioxide, J. Phys. Chem. 91 (1987) 3328–3333.
[12] P. Qu, J. Zhao, T. Shen, H. Hidaka, TiO_2-assisted photodegradation of dyes: a study of two competitive primary processes in the degradation of RB in an aqueous TiO_2 colloidal solution, J. Mol. Catal. A: Chem. 129 (1998) 257–268.
[13] N. San, A. Hatipoğlu, G. Koctürk, Z. Cinar, Prediction of primary intermediates and the photodegradation kinetics of 3-aminophenol in aqueous TiO_2 suspensions, J. Photochem. Photobiol. A: Chem. 139 (2001) 225–232.
[14] N. San, A. Hatipoğlu, G. Koctürk, Z. Cinar, Photocatalytic degradation of 4-nitrophenol in aqueous TiO_2 suspensions: theoretical prediction of the intermediates, J. Photochem. Photobiol. A: Chem. 146 (2002) 189–197.
[15] N. Strataki, V. Bekiari, E. Stathatos, P. Lianos, Effect of aggregation of dyes adsorbed on nanocrystalline titania films on the efficiency of photodegradation, J. Photochem. Photobiol. A: Chem. 191 (2007) 13–18.
[16] J.P.S. Valente, P.M. Padilha, A.O. Florentino, Studies on the adsorption and kinetics of photodegradation of a model compound for heterogeneous photocatalysis onto TiO_2, Chemosphere 64 (2006) 1128–1133.
[17] F. Zhang, J. Zhao, T. Shen, H. Hidaka, E. Pelizzetti, N. Serpone, TiO_2-assisted photodegradation of dye pollutants. II. Adsorption and degradation kinetics of eosin in TiO_2 dispersions under visible light irradiation, Appl. Catal. B: Environ. 15 (1998) 147–156.
[18] M.A. Hasnat, I.A. Siddiquey, A. Nuruddin, Comparative photocatalytic studies of degradation of a cationic and an anionic dye, Dyes Pigments 66 (2005) 185–188.
[19] J. Zhao, T. Wu, K. Wu, K. Oikawa, H. Hidaka, N. Serpone, Photoassisted degradation of dye pollutants. 3. Degradation of the cationic dye rhodamine B in aqueous anionic surfactant/TiO_2 dispersions under visible light irradiation: evidence for the need of substrate adsorption on TiO_2 particles, Environ. Sci. Technol. 32 (1998) 2394–2400.
[20] M.S. Chiou, G.S. Chuang, Competitive adsorption of dye metanil yellow and RB15 in acid solutions on chemically cross-linked chitosan beads, Chemosphere 62 (2006) 731–740.
[21] A.R. Cestari, E.F.S. Vieira, A.G.P.D. Santos, J.A. Mota, V.P.D. Almeida, Adsorption of anionic dyes on chitosan beads. 1. The influence of the chemical structures of dyes and temperature on the adsorption kinetics, J. Colloid Interface Sci. 280 (2004) (2004) 380–386.
[22] A.C. Chao, S.S. Shyu, Y.C. Lin, F.L. Mi, Enzymatic grafting of carboxyl groups on to chitosan—to confer on chitosan the property of a cationic dye adsorbent, Bioresour. Technol. 91 (2004) 157–162.
[23] Y. Twu, H. Huang, S. Chang, S. Wang, Preparation sorption activity of chitosan/cellulose blend beads, Carbohyd. Polym. 54 (2003) 425–430.
[24] W.L. Yan, R. Bai, Adsorption of lead and humic acid on chitosan hydrogel beads, Water Res. 39 (2005) 688–698.
[25] I.G. Lalov, I.I. Guerginov, M.A. Krysteva, K. Fartsov, Treatment of waste water from distilleries with chitosan, Water Res. 34 (5) (2000) 1503–1506.
[26] K. Yoshizuka, Z. Lou, K. Inoue, Silver-complexed chitosan microparticles for pesticide removal, React. Funct. Polym. 44 (2000) 47–54.
[27] M.S. Chiou, H.Y. Li, Adsorption behavior of reactive dye in aqueous solution on chemical cross-linked chitosan beads, Chemosphere 50 (2003) 1095–1105.
[28] M.S. Chiou, P.Y. Ho, H.Y. Li, Adsorption of anionic dyes in acid solutions using chemically cross-linked chitosan beads, Dyes Pigments 60 (2004) 69–84.
[29] F.C. Wu, R.L. Tseng, R.S. Juang, Enhanced abilities of highly swollen chitosan beads for color removal and tyrosinase immobilization, J. Hazard. Mater. B81 (2001) 167–177.
[30] D. Chen, A.K. Ray, Removal of toxic metal ions from wastewater by semiconductor photocatalysis, Chem. Eng. Sci. 56 (2001) 1561–1570.
[31] V. Augugliaro, C. Baiocchi, A.B. Prevot, E. García-López, V. Loddo, S. Malato, G. Marcí, L. Palmisano, M. Pazzi, E. Pramauro, Azo-dyes photocatalytic degradation in aqueous suspension of TiO_2 under solar irradiation, Chemosphere 49 (2002) 1223–1230.
[32] Z. Zainal, L.K. Hui, M.Z. Hussein, A.H. Abdullah, I. Hamadneh, Characterization of newly prepared TiO_2–chitosan/glass for the removal of a monoazo dye via the combination effect of photodegradation–adsorption, in: Proceedings of the International Advanced Technology Congress 2005-Conference on Advanced Materials, 2005, pp. 106–118.
[33] B. Tryba, A.W. Morawski, M. Inagaki, A new route for preparation of TiO_2-mounted activated carbon, Appl. Catal. B: Environ. 46 (2003) 203–208.
[34] R. Fretwell, P. Douglas, An active, robust and transparent nanocrystalline anatase TiO_2 thin film—preparation, characterization and the kinetics of photodegradation of model pollutants, J. Photochem. Photobiol. A: Chem. 143 (2001) 229–240.
[35] Z. Zainal, L.K. Hui, M.Z. Hussein, Y.H. Taufiq-Yap, I. Ramli, Removal of dyes using immobilized titanium dioxide illuminated by fluorescent lamps, J. Hazard. Mater. B125 (2005) 113–120.

[36] O.A.C. Monteiro Jr., C. Airoldi, Some thermodynamic data on copper-chitin and copper–chitosan biopolymer interactions, J. Colloid Interface Sci. 212 (1999) 212–219.
[37] Y.S. Ho, G. McKay, The kinetics of sorption of divalent metal ions onto sphagnum moss peat, Water Res. 34 (3) (2000) 735–742.
[38] T.A. McMurray, J.A. Byrne, P.S.M. Dunlop, J.G.M. Winkelman, B.R. Eggins, E.T. McAdams, Intrinsic kinetics of photocatalytic oxidation of formic and oxalic acid on immolised TiO_2 films, Appl. Catal. A: Gen. 262 (2004) 105–110.
[39] Y.M. Wang, S.W. Liu, Z. Xiu, X.B. Jiao, X.P. Cui, J. Pan, Preparation and photocatalytic properties of silica gel-supported TiO_2, Mater. Lett. 60 (2006) 974–978.
[40] B. Neppolian, H.C. Choi, S. Sakthivel, B. Arabindoo, V. Murugesan, Solar light induced and TiO_2 assisted degradation of textile dye reactive blue 4, Chemosphere 46 (2002) 1173–1181.
[41] W. Baran, A. Makowski, W. Wardas, The effect of UV radiation absorption of cationic and anionic dye solutions on their photocatalytic degradation in the presence TiO_2, Dyes Pigments 76 (2008) 226–230.